

# Real-time nondestructive citrus fruit quality monitoring system: development and laboratory testing

M. Yamakawa<sup>1</sup>, L. R. Khot<sup>2</sup>, R. Ehsani<sup>2\*</sup>, N. Kondo<sup>1</sup>

(1. *Division of Environmental Science and Technology, Kyoto University, Sakyo-ku, Kyoto, Japan;*

2. *University of Florida, IFAS, Citrus Research and Education Center, Lake Alfred, Florida, 33850, USA*)

**Abstract:** This study reports on the development and laboratory testing of the nondestructive citrus fruit quality monitoring system. Prototype system consists of a light detection and ranging (LIDAR) and visible-near infrared spectroscopy sensors installed on an inclined conveyer for real-time fruit size and total soluble solids (TSS) measurement respectively. Laboratory test results revealed that the developed system is applicable for instantaneous fruit size ( $R^2 = 0.912$ ) and TSS ( $R^2 = 0.677$ , standard error of prediction = 0.48 °Brix) determination. Future applications of such system would be in precision farming for in-field orange quality determination during the harvest and for row specific yield mapping and monitoring.

**Keywords:** LIDAR sensor, visible-near infrared spectroscopy, fruit size, sugar content

**Citation:** Yamakawa, M., L. R. Khot, R. Ehsani, and N. Kondo. 2012. Real-time nondestructive citrus fruit quality monitoring system: development and laboratory testing. *Agric Eng Int: CIGR Journal*, 14(3): 117–124.

## 1 Introduction

Quantifying citrus fruits quality is important in grading fruits and establishing their market price. It provides consumers with quality information of a particular produce (Aleixos et al., 2002). Traditionally, fruit size used to be measured using sizing ring (Food and Agriculture Organization of the United Nations [FAO], 1989), drum-type grading machine (Reyes, 1988) and light blocking type grading machine (Umeda, 1976). Above approaches enabled the classification of fruits based on their size. Since then, image processing techniques have been established allowing not only the size measurements but also the nondestructive determination of blemish and color of the fruits (Kondo et al., 2006). Moreover, sugar content, total soluble solids (TSS) of citrus could also be measured using NIR spectroscopy (Kawano, Fujiwara, and Iwamoto, 1993). Recently, Kondo et al. (2009), and Kurita et al. (2009)

have developed technique for detecting rotten oranges by identifying fluorescence substance present in the orange skin. Similarly, Slaughter et al. (2008) reported the use of the fluorescence technique to detect freeze damage in oranges. These technologies are being used in packing houses.

Currently, attempts are being made to measure the fruit quality in the field after harvest, for precision agriculture applications. Kohno et al. (2011) reported the development of a real-time in-field “Mobile citrus grading machine”, which grades citrus fruits based on their size and color (using imaging technique), and sugar content and acidity measured using on-board near infrared spectrometer. A global positioning system (GPS) receiver attached to this machine can be used to geo-reference the in-field fruit grading. Moreover, 3-D field maps can be created using the acquired information from this mobile citrus grading machine (Yamakawa et al., 2010).

The post-harvest fruit quality monitoring system can also be useful for estimating the number of fruits per harvest row or fruits per unit area and determining the

**Received date:** 2012-03-21 **Accepted date:** 2012-06-30

\* **Corresponding author:** R. Ehsani, E-mail: [ehsani@ufl.edu](mailto:ehsani@ufl.edu), Phone: 1-863-956-8770, Fax: 1-863-956-4631.

time of harvest that dictates the fruit quality. Furthermore, the economics of fruit sale can be improved based on their quality. Researchers at the University of Florida have developed the field-based plant material removal and fruit cleaning system (Ehsani, 2011). This system can remove unwanted plant materials, branches and stems attached to the harvested fruits, and can have several sensors on-board that can be used for fruit quality determination. Therefore, this research was focused on the development of a portable system that can nondestructively measure post-harvest citrus fruit size and TSS. Such system would be part of the on-board sensors of the in-field plant material removal and citrus fruit cleaning system for citrus quality monitoring. This

study reports on the prototype development and laboratory testing of such unit for automated fruit quality determination.

## 2 Prototype fruit quality monitoring system

Prototype fruit quality monitoring system (Figure 1) consisted of light detection and ranging (LIDAR) sensor and near-infrared spectroscopy probe mounted on inclined conveyor (mimicking the in-field system conditions), a data logging computer and fruit quality determination algorithms. Laser rangefinder (UTM-30LX, Hokuyo Automatic Co., Ltd., Osaka, Japan), henceforth termed as LIDAR sensor, was used to measure the fruit size.

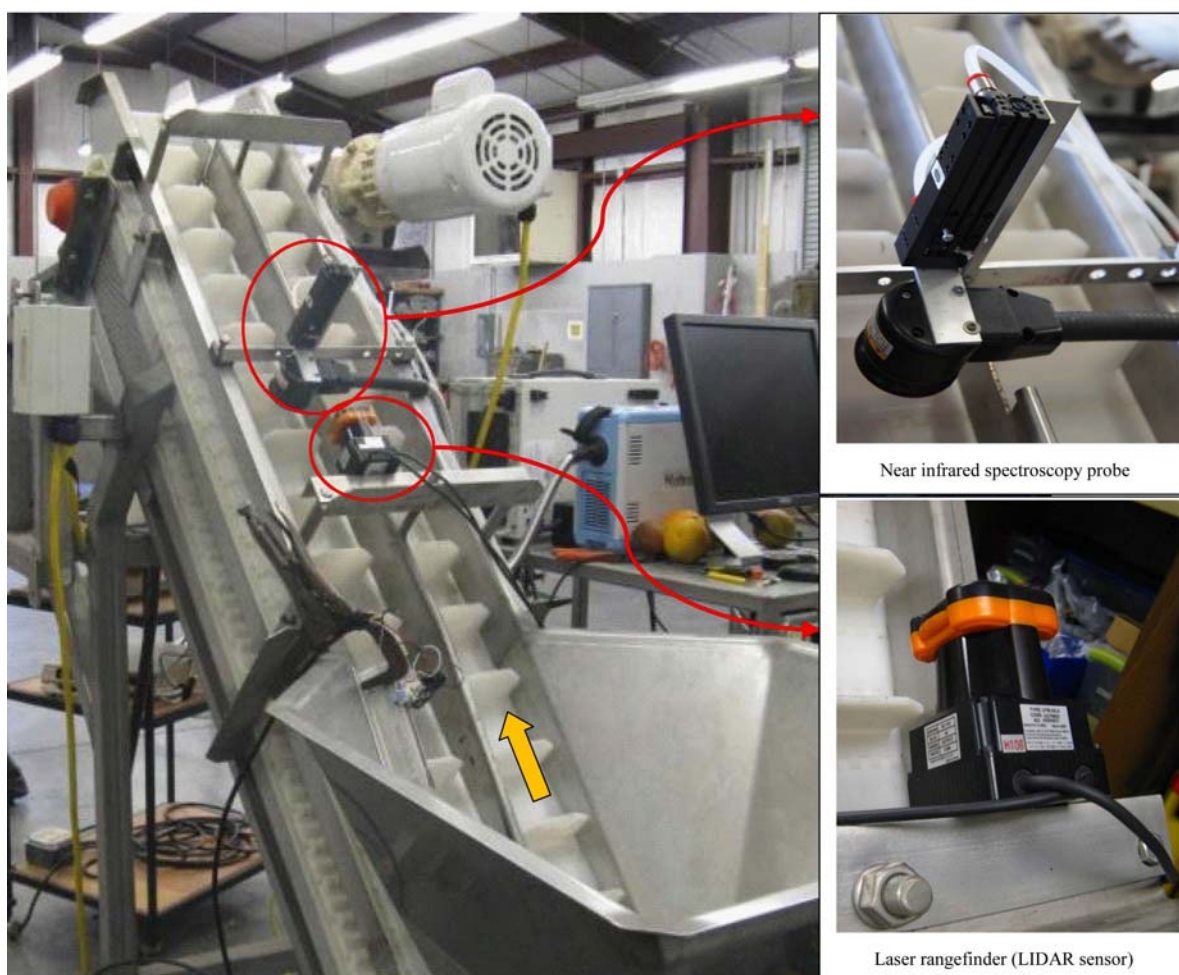


Figure 1 Citrus fruit quality measurement system

The LIDAR sensor was attached to an inclined conveyor (Figure 1) procured from Heinzen Manufacturing International, Gilroy, CA. Sensor consisted of a near infrared laser (905 nm) with a two dimensional scan range of 0-270°. It was used at

angular resolution of 0.25° that resulted in response time of about 25 ms.

Near-infrared (NIR) spectroscopy based portable nondestructive sugar content measurement device (K-BA100R, Kubota Corporation, Osaka, Japan), shown

in Figure 1, was used to measure TSS of the fruits. This device consists of a probe and main unit, and measures TSS of a fruit when the probe touches the fruit skin. It uses certain absorption band in NIR region related to specific functional group (mainly -OH, -CH and -NH). The NIR spectroscopy based transmission method acquires only surface information whereas the reflection method needs large amount of energy for light to pass through the fruit. Therefore, a new measuring probe developed by the manufacturer was used in this study. This probe consisted of ring light arranged in a concentric pattern and centrally-located light receiving fiber. Light emitted from the ring light goes through the sample and spreads inside the sample. Later, it was detected by light receiving fiber and the data was passed to the main unit. This device can measure and indicate TSS of fruits with calibration curve downloaded into this device. Data from sensor can also be used to establish the relational expression between absorbance and concentration as shown in Morimoto (2003) and Nicolai et al. (2007). Moreover, device can also be used as the NIR spectrometer. It can measure absorbance in every 2 nm from 600-1,000 nm. In this wavelength range, absorbance is weak and transmittance is strong. Thus, this wavelength is usually used for measuring transmission spectra of food with high water content (Iwamoto, Kawano, and Uozumi, 1994; Morimoto, 2003; Fujiwara, 2004; Kondo, 2007).

Figure 2 outlines the detailed steps followed in laboratory during the evaluation of the fruit quality monitoring system. The inclined conveyor, set to a travel speed of about 26 cm/s, carried the fruits from bottom hopper. As shown in the flow chart: firstly, fruit size (diameter in mm) was measured while the fruit passed under the LIDAR sensor. Following the size measurement, NIR sensor probe measured the TSS of a fruit. The fruit was then moved forward. These steps were repeated until all fruits in hopper were sensed by the system. Division of each compartment of the inclined conveyor was detected by a switch. Fruits were placed in the center using two small bars. The inclined conveyor was controlled by programmable logic controller (PLC). The LIDAR and TSS sensors were

programmed using LabVIEW 8.5<sup>®</sup> (National Instrument, Austin, TX, USA).

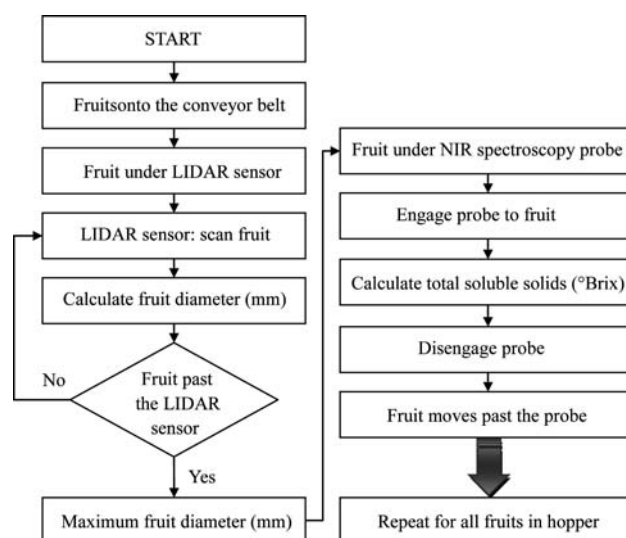


Figure 2 Operational flowchart of fruit size and total soluble solids measurement system

## 2.1 Fruit size measurement

Maximum diameters of the fruits were measured in this study. LIDAR sensor scanning interval was set to 50 ms. Angle setting of the LIDAR sensor was from  $-25^{\circ}$  to  $+25^{\circ}$  such that the sensor avoided the division lane detection on either side of the fruit. Distance threshold value was set at 180 mm and the data less than 180 mm was used to calculate the distance between the extreme-right and -left point of the fruit as shown in Figure 3. Scanning was performed several times for each fruit to calculate the distance between the extreme-right and -left points. Maximum distance was regarded as the diameter of the fruit. A custom program was written in LabVIEW<sup>®</sup> to control and log the data from the LIDAR sensor. Fruits were distinguished using the switch that could detect the white dividers between them on the conveyor.

## 2.2 Sugar content measurement

To measure the TSS of fruits coming through the inclined conveyor automatically, the fruit selector probe was installed as shown in Figure 1 (right bottom). Mini ball rail slide (DLM-07M-50, De-Sta-Co, Auburn Hills, MI), controlled by pneumatic pressure, was used to engage and disengage the probe over the fruit. Programmable controller (FP0-C14RS, Panasonic Corporation, Erlanger, KY) and pneumatic directional

control valves (R432015593, Bosch Rexroth, Charlotte, NC) were used to control the pneumatic pressure. The procedure of the sugar content measurement involved: stoppage of fruit under the probe; engage the probe with

fruit underneath; measure and record the absorbance spectra for each fruit. Following this, the probe retracted to its initial position, and then the conveyor moved up until next fruit is detected.

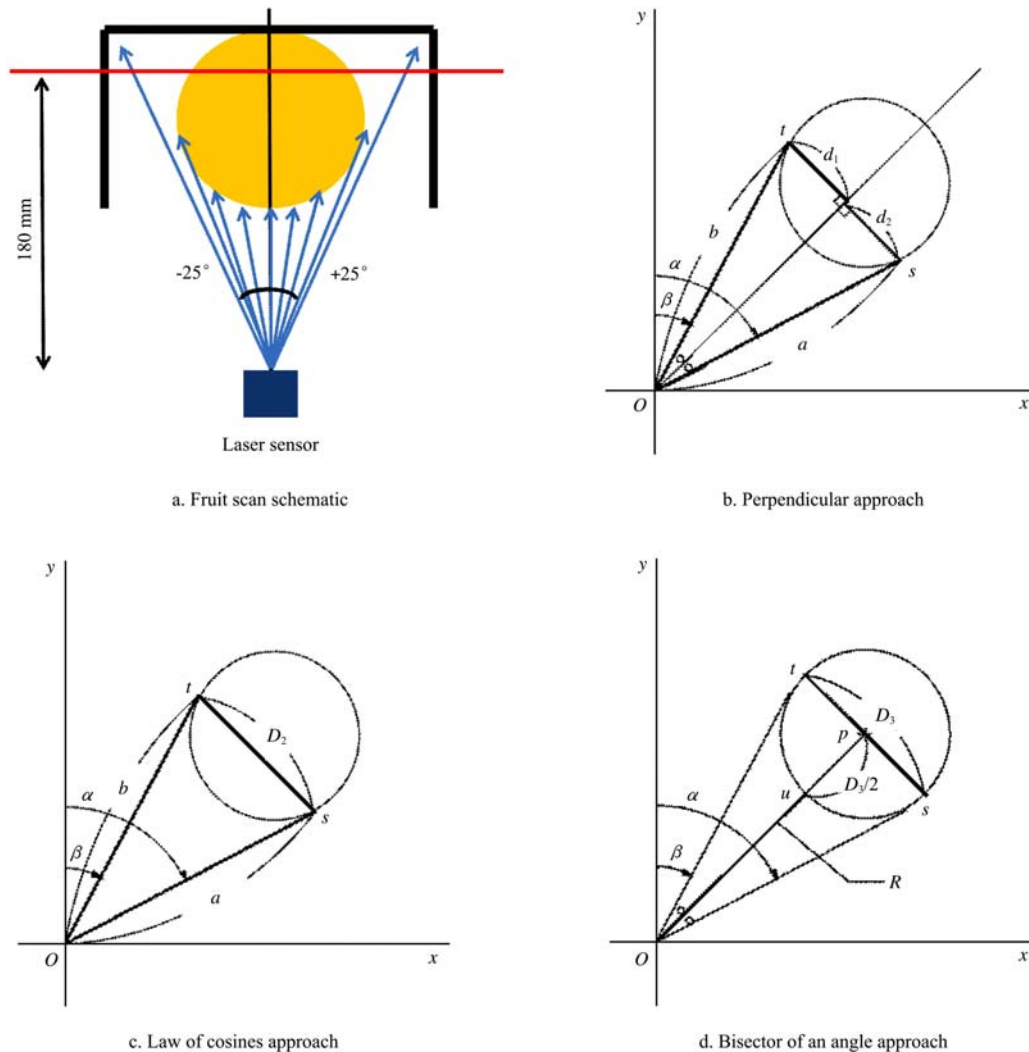


Figure 3 LIDAR sensor based fruit size measurement

### 3 Materials and methods

In this study, oranges (variety: Valencia) harvested during March 2011 from Citrus Research and Education Center (CREC), University of Florida orchards were used for the calibration and laboratory testing of the system. Fruits were put into the hopper connecting inclined conveyer and the maximum diameter and TSS were automatically measured using the sensors on-board. During the calibration, 10 oranges were placed randomly, rightward, leftward and centrally to measure the fruit size twice for each fruit. This procedure was repeated eight times on same fruits and the average fruit size (mm) was

used in further analysis. Actual fruit sizes were also measured using the caliper and were compared with the fruit size estimates.

Three methods of diameter estimations were compared in this study to determine the most accurate method for measuring the fruit diameter. Following labels were used for calculating diameter (Figure 3):  $s$  - extreme right point of an orange that the LIDAR sensor detected;  $t$  - extreme left point;  $o$  - point of the LIDAR sensor;  $a$  - the distance of the line  $o-s$ ;  $b$  - distance of the line  $o-t$ ;  $\alpha$  is the angle from  $y$  axis to line  $o-s$ ; and  $\beta$  is the angle from  $y$  axis to line  $o-t$ .

Equations (1) – (3) describe the diameter calculation

approaches that use ‘perpendicular line’, ‘law of cosines’ and ‘bisector of an angle’ respectively. In perpendicular line approach, fruit diameter ( $D_1$ ) was calculated as:

$$D_1 = d_1 + d_2 = a \sin \frac{\alpha - \beta}{2} + b \sin \frac{\alpha - \beta}{2} \quad (1)$$

The equation above uses the perpendicular line from the tangent point, “s” and “t” to the bisector of an  $\angle tos$ . With law of cosines, fruit diameter ( $D_2$ ) was calculated as:

$$D_2 = \sqrt{a^2 + b^2 - 2ab \cos(\alpha - \beta)} \quad (2)$$

This formula uses the law of cosines with  $\Delta ots$ . Using bisector of an angle technique, fruit diameter ( $D_3$ ) was calculated as:

$$D_3 = \frac{2R \tan \frac{\alpha - \beta}{2}}{1 - \frac{\alpha - \beta}{2}} \quad (3)$$

Equation (3) assumes that fruit is a circle and that line  $s-t$  intersects the middle of the fruit. The vertex of bisector of an  $\angle tos$  and the circle is  $u$ . The distance of line  $o-u$  is  $R$ .

TSS measurement system probe was attached to the orange surface and covered with a black cloth. Absorbance spectra of the 70 fruits were measured using this probe. A total of 50 oranges were used for calibration and 20 were used for validation. Spectral measurement of each fruit was repeated for 10 times. To develop a calibration curve, TSS of each orange was measured, °Brix or %, with a portable refractometer (Thermo Fisher Scientific Inc., USA). This unit measured TSS in the range of 28-62 °Brix with an accuracy of 0.2 °Brix.

Statistical analysis software, SAS (ver. 9.2, SAS Institute Inc., Cary, NC) was used for extracting significant features related to TSS estimation. During spectral analysis of the data, secondary differentiation of absorbance in 700 nm to 980 nm range was used as an explanatory variable, and the value from the portable refractometer was used as an objective variable. Twenty wavelengths that significantly contributed to the relationship between the spectra and the portable refractometer based TSS data were chosen using regression analysis technique (‘PORC REG’). From the

20 wavelengths, wavelengths that highly correlated to the sugar content were selected with stepwise multiple linear regression technique that used ‘forward selection’ option. In forward selection, a spectral feature is added sequentially until there is no further improvement in regression fits. Finally, the calibration curve was developed and validated. Most appropriate calibration curve was made based on standard error of calibration (SEC), standard error of prediction (SEP) and ‘Bias’, which were calculated as below (Equations (4) – (6)).

$$SEC = \sqrt{\frac{\sum (y_i - \hat{y}_i)^2}{(N_c - p - 1)}} \quad (4)$$

$$SEP = \sqrt{\frac{\sum (y_i - \hat{y}_i - Bias)^2}{(N_p - 1)}} \quad (5)$$

$$Bias = \frac{1}{N_p} \sum (\bar{y}_i - \hat{y}_i) \quad (6)$$

In these equations,  $y_i$  is the measured value from refractometer;  $\hat{y}_i$  is the predicted value;  $N_c$  is the number of the samples for calibration;  $N_p$  is the number of the samples for validation and  $p$  is the number of the wavelength of the calibration curve (Iwamoto, Kawano, and Uozumi, 1994; Kobayashi, Tallada, and Nagata, 2005).

Fruit size and TSS estimation approaches were later tested with 30 fresh oranges. Test fruits consisted of varied orange sizes, i.e., 10 small, 10 medium and 10 large sized fruits. During testing, each orange size was measured 10 times and averages were considered for regression analysis.

## 4 Results and discussion

Table 1 summarizes the descriptive statistics on actual fruit size and TSS of the citrus fruits used for calibration, validation and testing of the prototype system. Linear regression of the actual and estimated fruit size measurements showed that the ‘law of cosine’ approach had better fit ( $y = 0.71x + 15.04$ ,  $R^2 = 0.935$ ) than either of the ‘perpendicular line’ approach ( $y = 0.72x + 15.12$ ,  $R^2 = 0.915$ ) or the ‘bisector of an angle’ approach ( $y = 0.63x + 22.29$ ,  $R^2 = 0.875$ ). Therefore, the ‘law of cosine’ approach was used for fruit size estimation during further testing of the system. Figure 4 shows regression fit between actual and estimated fruit size of 30 fruits

used for the testing of the system. Evidently, LIDAR sensor based fruit size estimates had good fit with actual fruit size data ( $R^2 = 0.912$ ). Thus, fruit size estimation component of the system is ready to be used as an embedded part of a field-based plant material removal and fruit cleaning system.

**Table 1** Descriptive statistics on fruits used for size and total soluble solids measurements

	Samples	Min	Max	Mean	Std. Dev.
Fruit size / mm					
Calibration	10	66	82	72	6
Testing	30	60	88	71	8
TSS / °Brix					
Calibration	50	12	15	14	1
Validation	20	10	15	13	1
Testing	30	10	17	13	2

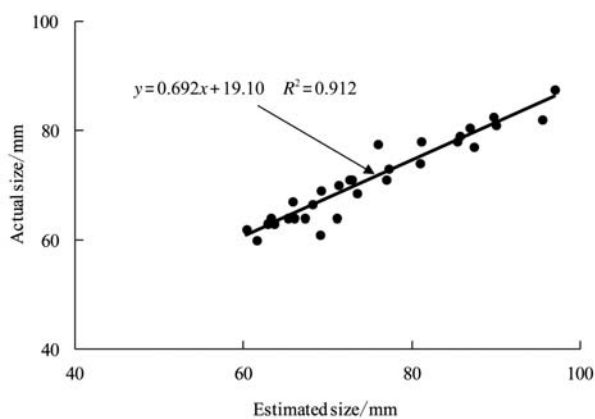
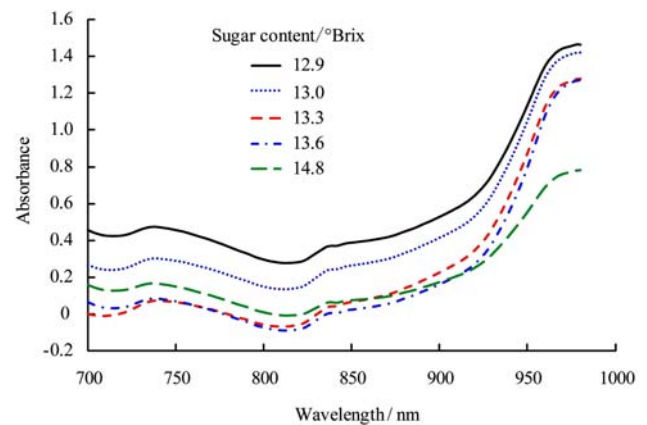


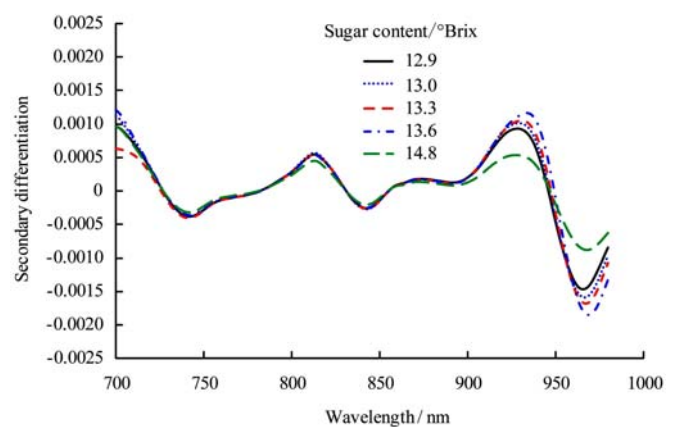
Figure 4 Actual and estimated size of fruits tested using the developed system

Figure 5a shows the NIR spectroscopy based typical spectral signatures of citrus fruits with varied levels of TSS. Secondary differentiation features for identical signatures were as shown in Figure 5b. From total of 141 bands in the wavelength ranges of 728-920 nm, 20 bands were significantly related (at 5% level) to the TSS with model fit  $R^2$  of 0.952. Multiple linear regression analysis further narrowed the selection to 12 spectral bands, i.e., 728, 750, 784, 788, 792, 804, 884, 886, 894, 900, 914, and 920 nm. These feature based sugar content estimates and actual sugar content data had good fit with coefficient of determination (calibration),  $R^2 = 0.805$  ( $SEC = 0.33$  °Brix). Similarly, the actual and estimated sugar content from validation dataset had good

fit with  $R^2 = 0.707$  ( $SEP = 0.48$  °Brix,  $Bias = 0.44$ ).



a. Raw absorbance for citrus fruits with different levels of TSS



b. Resulting secondary differences of spectral signatures

Figure 5 Typical raw absorbance and resulting secondary differences of spectral signatures for citrus fruits with different levels of TSS

Figure 6 shows the actual and NIR spectroscopy based TSS estimates of fruits tested using the developed system. The TSS estimates showed good fit ( $R^2 = 0.677$ ) with actual TSS, but further improvements for practical applications are needed. Three key issues discussed below need to be resolved to have improved TSS estimation. First is the probe arm design. It was observed that the probe, with fixed engage-disengage arm position, had better grip on big sized oranges than on the smaller ones. Thus, an arm system that can fit varied sizes need to be built. The second issue is related to the thickness of fruits that increased the sugar content measurement time. For the fruits tested in this study, each fruit was under the probe for about 90 s for measurement. The lamp with stronger output power might resolve this problem. Lastly, establishing better

calibration curve, on more comprehensive sample datasets, could enable more accurate measurements.

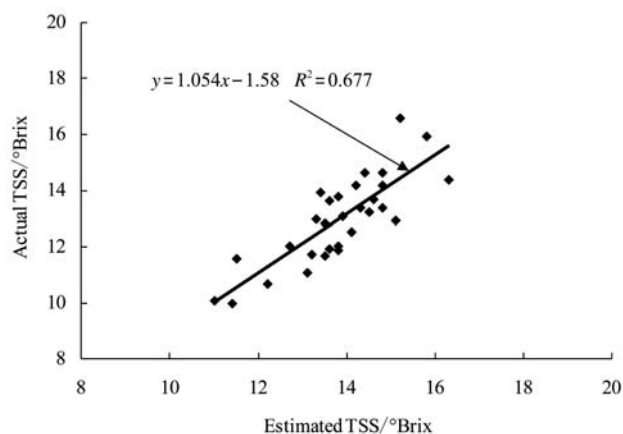


Figure 6 Relationship between actual and estimated TSS of fruits tested using the developed system

Researchers have used fourier transform NIR (Lu et al., 2006), visible NIR (Liu et al., 2010; Antonucci et al., 2011) spectrometers for nondestructive TSS measurements of citrus fruits. Lu et al. (2006) used fourier transform based NIR spectrometer for nondestructive TSS estimation of citrus (variety: Gannan) fruits. In their study, partial-least square (PLS) calibration and prediction models showed good fit with measured TSS with  $R^2 = 0.990$  and  $0.707$  respectively. System test results of TSS estimation obtained in this study are comparable with the prediction results obtained in their study. Also, this study used NIR spectrometer, a less expensive and portable technique than FTIR-NIR spectrometer, which would be part of the in-field fruit quality measurement system. Antonucci et al. (2011) also used visible NIR spectrometer for TSS estimation of oranges. They reported that the linear regression models had good fits with  $R^2 = 0.723$  and  $0.706$  on spectral data from “Miho” Satsuma and “Page” mandarin varieties respectively. Despite the inconformity, the results from this study are comparable with Antonucci et al. (2011). Nonetheless, prototype system developed herein needs to be tested to acquire more spectra so that a robust

calibration equations can be developed.

In this study, the multiple linear regression approach was used for calibration and validation models development. Liu et al. (2010) reported various linear and non-linear multivariate regression approaches of spectral data analysis and for spetras acquired using visible NIR diffuse reflectance spectroscopy in the wavelength range of 450-1,750 nm on “Gannan” navel oranges. They used multiple linear regression, principal component regression, PLS, Poly-PLS and Spline-PLS models on the spectral data preprocessed using techniques such as average smoothing, multiplicative scatter correction, and first and second derivatives. Among the above prediction models, Spline-PLS was found superior with  $R^2 = 0.757$  and prediction error, *SEP* of  $0.47$  °Brix. Results obtained in this study also had equivalent prediction error with *SEP* of  $0.48$  °Brix. Nonetheless, in further data analysis, various other prediction models would also be evaluated to assess the better models with less prediction errors.

## 5 Conclusions

In this study, a prototype unit was successfully developed and tested under laboratory conditions for automated and nondestructive citrus fruit quality monitoring. Test results confirmed the usefulness of such system with good regression fit of estimated and actual fruit size ( $R^2 = 0.91$ ), and TSS measurements ( $R^2 = 0.68$ , *SEP* =  $0.48$  °Brix). Further studies are needed to improve the NIR spectroscopy based TSS estimation. Also, the system needs to be tested for other citrus varieties under laboratory conditions for developing a variety of specific calibration curves of TSS estimations. Upon successful laboratory testing, this system will be incorporated in a field-based plant material removal and fruit cleaning system developed at the University of Florida for in-field fruit size and sugar content monitoring.

## References

- Aleixos, N., J. Blasco, F. Navarrón, and E. Moltó. 2002. Multispectral inspection of citrus in real-time using machine vision and digital signal processors. *Computers and Electronics in Agriculture*, 33 (2): 121-137.
- Antonucci, F., F. Pallottino, G. Paglia, A. Palma, S. D'Aquino, and P. Menesatti. 2011. Non-destructive estimation of mandarin maturity status through portable VIS-NIR spectrophotometer. *Food Bioprocess Technology*, 4 (5): 809-813.
- Ehsani, R. 2011. Mass harvesters: trash removal system development. Available at: <http://citrusmh.ifas.ufl.edu/index.asp?s=7&p=6>. Accessed on: 10/29/2011.
- Food and Agriculture Organization of the United Nations [FAO]. 1989. Prevention of postharvest food losses: fruits, vegetables and root crops. FAO training series no. 17/2, pp.157.
- Fujiwara, T. 2004. General problems in application of near infrared spectroscopy to measurement of sugar and acid contents in fruits. *Japan Journal of Food Engineering*, 5 (2): 51-62.
- Lu, H.-S., H.-R. Xu, Y.-B. Ying, X.-P. Fu, H.-Y. Yu, and H.-Q. Tian. 2006. Application Fourier transform near infrared spectrometer in rapid estimation of soluble solids content of intact citrus fruits. *Journal of Zhejiang University Science B*, 7 (10): 794-799.
- Iwamoto, M., S. Kawano, and J. Uozumi. 1994. *Introduction of near-infrared spectroscopy*. Tokyo, Japan: Saiwai Shobou.
- Kawano, S., K. Fujiwara, and M. Iwamoto. 1993. Nondestructive determination of sugar content in Satsuma mandarin using near infrared (NIR) transmittance. *Journal of Japanese Society of Horticultural Science*, 62 (2): 465-470.
- Kobayashi, T., J. Tallada, and M. Nagata. 2005. Basic study on measurement of sugar content for citrus unshiu fruit using NIR spectrophotometer. *Bulletin of the Faculty of Agriculture, Miyazaki University Journal Article*, 51 (1): 1-8.
- Kohno, Y., N. Kondo, M. Iida, M. Kurita, T. Shiigi, Y. Ogawa, T. Kaichi, and S. Okamoto. 2011. Development of a mobile grading machine for citrus fruit. *Engineering in agriculture, Environment and Food*, 4 (1): 7-11.
- Kondo, M. 2007. Food analysis by near-infrared spectroscopy. *Bulletin of Nagoya Bunri University*, 7: 23-28.
- Kondo, N., M. Kuramoto, H. Shimizu, Y. Ogawa, M. Kurita, T. Nishizu, V. Kiong Chong, and K. Yamamoto. 2009. Identification of fluorescent substance in mandarin orange skin for machine vision system to detect rotten citrus fruits. *Engineering in agriculture, Environment and Food*, 2 (2): 54-59.
- Kondo, N., M. Monta, N. Noguchi, O. Yukumoto, Y. Matsuo, Y. Ogawa, T. Fujiura, and S. Arima. 2006. *Agri-Robot (II)-Mechanisms and Practice*, 26-27 & 58-59.
- Kurita, M., N. Kondo, H. Shimizu, P. P. Ling, P. D. Falzea, T. Shiigi, K. Ninomiya, T. Nishizu, and K. Yamamoto. 2009. A double image acquisition system with visible and UV LEDs for citrus fruit. *Journal of Robotics and Mechatronics*, 21 (4): 533-540.
- Liu, Y., X. Sun, J. Zhou, H. Zhang, and C. Yang. 2010. Linear and nonlinear multivariate regressions for determination sugar content of intact Gannan navel orange by Vis-NIR diffuse reflectance spectroscopy. *Mathematical and Computer Modeling*, 51 (11-12): 1438-1443.
- Morimoto, S. 2003. Portable non-destructive quality measurement device for fruits. *Inspection engineering*, 8(6): 58-63.
- Nicolai, B. M., K. Beullens, E. Bobelyn, A. Peirs, W. Saeys, K. I. Theron, and J. Lammertyn. 2007. Nondestructive measurement of fruit and vegetable quality by means of NIR spectroscopy: a review. *Postharvest Biology and Technology*, 46 (2): 99-118.
- Reyes, M. U. (Ed.). 1988. *Design Concept and Operation of ASEAN Packinghouse Equipment for Fruits and Vegetables*. Postharvest Horticulture Training and Research Center, University of Los Baños, College of Agriculture, Laguna, Philippines.
- Slaughter, D. C., D. M. Obenland, J. F. Thompson, M. L. Arpaia, and D. A. Margosan. 2008. Non-destructive freeze damage detection in oranges using machine vision and ultraviolet fluorescence. *Postharvest Biology and Technology*, 48 (3): 341-346.
- Umeda, S. 1976. Automatic sorting of agricultural products. *Journal of the Japanese Society of Agriculture Machinery*, 38 (3): 345-351.
- Yamakawa, M., Y. Kohno, N. Kondo, M. Iida, T. Shiigi, Y. Ogawa, and M. Kurita. 2010. 3-D maps of Japanese citrus information for precision agriculture. ASABE Paper Number: 1009880. St. Joseph, Mich.: ASABE.